JOURNAL OF GUIDANCE, CONTROL, AND DYNAMICS
Vol. 29, No. 3, May–June 2006

Parking a Spacecraft near an Asteroid Pair

Frederic Gabern,* Wang S. Koon,† and Jerrold E. Marsden‡
California Institute of Technology, Pasadena, California 91125

This paper studies the dynamics of a spacecraft moving in the field of a binary asteroid. The asteroid pair is modeled as a rigid body and a sphere moving in a plane, while the spacecraft moves in space under the influence of the gravitational field of the asteroid pair, as well as that of the sun. This simple model captures the coupling between rotational and translational dynamics. By assuming that the binary dynamics is in a relative equilibrium, a restricted model for the spacecraft in orbit about them is constructed that also includes the direct effect of the sun on the spacecraft dynamics. The standard restricted three-body problem (RTBP) is used as a starting point for the analysis of the spacecraft motion. We investigate how the triangular points of the RTBP are modified through perturbations by taking into account two perturbations, namely, that one of the primaries is no longer a point mass but is an extended rigid body, and second, taking into account the effect of orbiting the sun. The stable zones near the modified triangular equilibrium points of the binary and a normal form of the Hamiltonian around them are used to compute stable periodic and quasi-periodic orbits for the spacecraft, which enable it to observe the asteroid pair while the binary orbits around the sun.

Nomenclature

$\mathcal{A}()$	=	mechanical connection
a_s	=	distance from the sun to the center of masses of the binary
G	=	universal constant of gravitation
$G_r()$	=	terms of degree r in the expansion of the generating function
$H()$	=	Hamiltonian function
$H_r()$	=	terms of degree r in the expansion of the Hamiltonian function
I_{zz}	=	inertia tensor of the rigid body
$\mathbb{I}()$	=	locked inertia tensor of the system
$J()$	=	momentum map
$K()$	=	kinetic energy function
$L()$	=	Lagrangian function
$L_{1,\ldots,5}$	=	Lagrangian points of the restricted three-body problem
L_4'	=	substitute of the L_4 Lagrangian point in the T model
M	=	mass of the rigid body
m	=	mass of the spherical body
m_s	=	mass of the sun
N	=	order of the normal form computations
$\mathcal{N}(I)$	=	normal form of the Hamiltonian in terms of action variables I
$PO(L_4')$	=	periodic orbit that substitutes the L_4 Lagrangian point in the T-model perturbed by the sun
$\mathcal{R}(I, \varphi, \theta_s)$	=	remaining part of the Hamiltonian that is not in normal form
r_L	=	distance between the asteroids forming the binary at the relative equilibrium
$SE(2)$	=	planar Euclidean group
$SO(2) = S^1$	=	group of rotations in the plane
T_L	=	period of the uniform rotation of the binary at the relative equilibrium
$V()$	=	potential energy function
μ	=	grade of mass dispersion of the rigid body
μ_{R}	=	Routh critical value
μ_{RTBP}	=	mass parameter of the restricted three-body problem
ν	=	mass parameter of the full two-body problem
ω_L	=	frequency of the uniform rotation of the binary at the relative equilibrium
ω_s	=	frequency of the the sun in the time-perturbed T model

Received 15 December 2004; revision received 29 March 2005; accepted for publication 29 March 2005.

*Postdoctoral Scholar, Control and Dynamical Systems, Caltech, 107-81; currently Lecturer, Matemàtica Aplicada I, Universitat Politècnica de Catalunya, Av. Diagonal, 647 08028 Barcelona, Spain.

†Senior Scientist and Lecturer, Control and Dynamical Systems, 107-81, Caltech.

‡Professor, Control and Dynamical Systems, 107-81, Caltech.

I. Introduction

In the last decade, many asteroid satellites and double asteroids have been discovered.[1] These include Dactyl, the first natural satellite of an asteroid ever found (see Fig. 1) and over 50 other binary asteroids.[2]

Therefore, the study of spacecraft motion about an asteroid pair is an extremely relevant topic for future missions to asteroids, because 16% of near-Earth asteroids (NEA) are thought to be binaries.[2] Binaries can be used as real-life laboratories to test rigid-body gravitational dynamics.[1] For instance, an important question is to find stable zones and orbits near the asteroid pair where a spacecraft can "park" to carry out measurements and observations of the binary as the pair orbits around the sun (see Fig. 2).

In solving this problem, we use the circular restricted three-body problem[3] (RTBP). The RTBP describes the motion of a massless particle under the gravitational attraction of two massive bodies (primaries) that presumably revolve in circular orbits around their common center of masses. Usually, the system is studied in a rotating frame (synodical), where the two massive bodies are fixed on the x axis. The details on how to derive the corresponding equations of motion can be found, for instance, in Ref. 3.

The RTBP has five equilibrium points (in synodical coordinates). Three of them are on the x axis, and they are known as collinear points or L_1, L_2, and L_3. The remaining two form equilateral triangles with the massive bodies and are known as triangular points or L_4 and L_5 (see Fig. 3).

Although the collinear points are always unstable, the stability of the triangular points depends on the value of $\mu_{\mathrm{RTBP}} = m/(M+m)$, where m and M are the masses of the primaries. If $\mu_{\mathrm{RTBP}} < \mu_R$, where $\mu_R = \frac{1}{2}[1 - \sqrt{(23/27)}]$ (known as the Routh critical value), the triangular points are spectrally stable; otherwise, they are unstable. These "equilateral" points are of interest to us because their stability properties will vary because of the rigid-body effects.

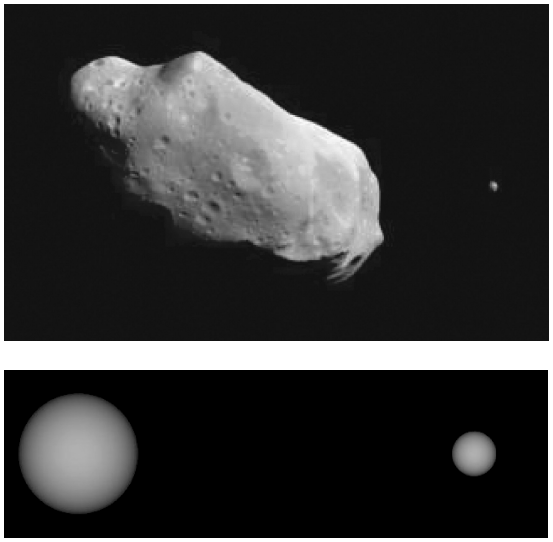

Fig. 1 Top: Ida and Dactyl (source: JPL); bottom: A schematic diagram representing the sizes of the 2000 DP107 components and their separation, drawn to scale (source: J. L. Margot, Caltech).

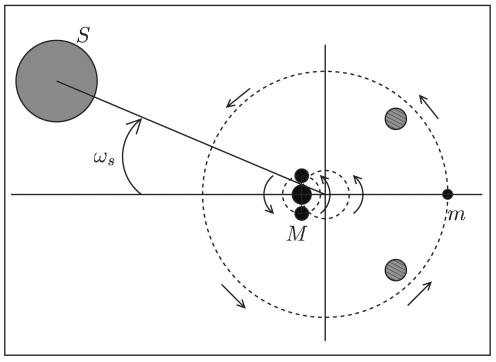

Fig. 2 Schematic diagram showing two stable zones for the spacecraft (gray ○) to observe the binary (*M* and *m*) as the asteroid pair orbits around the sun (*S*).

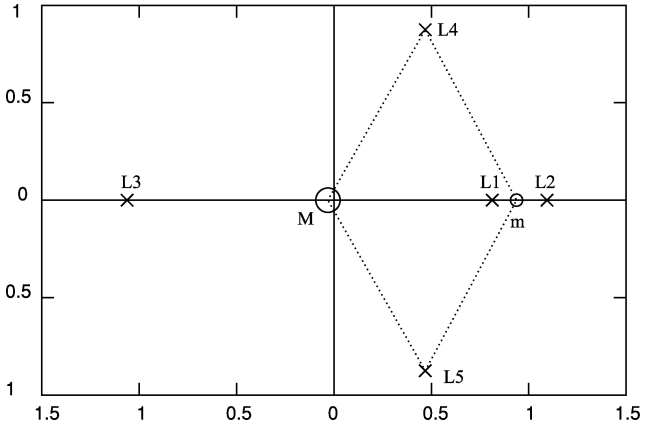

Fig. 3 Five equilibrium points of the RTBP.

The main aim of this paper is thus to study how these triangular equilibria are perturbed 1) when one of the primaries is an extended rigid body, and 2) when the effect of orbiting the sun is also considered. Under these situations, the coupling between the dynamics of the relative translational motion of the two bodies and the rigid-body rotation has to be taken into account. Furthermore, a time dependency will appear because of the perturbation of the sun.[4,5] Questions (1) and (2) are also addressed in Ref. 6 with a different methodology.

The collinear unstable points are also worth studying because we know, via Genesis Discovery Mission, for example, that it can be cheap to park a spacecraft near them by using the so-called center manifold.[7]

We use a simple model for the asteroid pair, a planar system made up of a rigid body and a sphere. This model is known as sphere restriction of the full two-body problem[8] (F2BP). The F2BP considers the gravitational interaction between two distributed bodies (see Ref. 9 for a formal definition of the problem and some initial stability studies, and see Refs. 10–12 for more studies on stability of the F2BP, including the sphere restriction case).

To model the spacecraft motion, we assume the binary to be in a relative equilibrium, and we also consider the direct effect of the sun on the spacecraft. Other studies in the literature[6,13] use the approach taken in Hill's problem, in which the sun is taken at infinity, to tackle the influence of the perturbation of the sun.

The basic techniques used in the present paper are taken from reduction theory and dynamical systems. The use of Hamiltonian reduction methods allows us to reduce the dimension of the problem and helps in the construction of the models. Normal Form techniques are central to our numerical explorations in studying these models. The software we used is adapted from the programs in Refs. 14 and 4, and it uses symbolic algebra routines to obtain high-order expansions (Taylor and Fourier–Taylor series) of the functions involved in the computations. These high-order expansions are important, for instance, to obtain relatively high inclination observation orbits for the spacecraft.

We first derive the reduced equations for the asteroid pair via reduction theory and make an analytical study of this reduced model. We then construct the models for the spacecraft motion based on a relative equilibrium solution of the asteroid pair. Only the direct effect of the sun on the spacecraft (and not on the asteroid pair) is considered in the modeling. Next, we study the dynamics of these models in the vicinity of the stable triangular points and use this study to find stable periodic and quasi-periodic orbits suitable for parking the spacecraft while it observes the binary. Finally, the conclusions are presented.

II. Model of the Asteroid Pair

To obtain a model of an asteroid pair, we apply Abelian reduction (see Refs. 15–17 for the details) to the particular case of the planar F2BP with the sphere restriction.

A. Equations of Motion for the Binary

Consider the mechanical system of a rigid body and a sphere that are moving in a plane, as in Fig. 4.

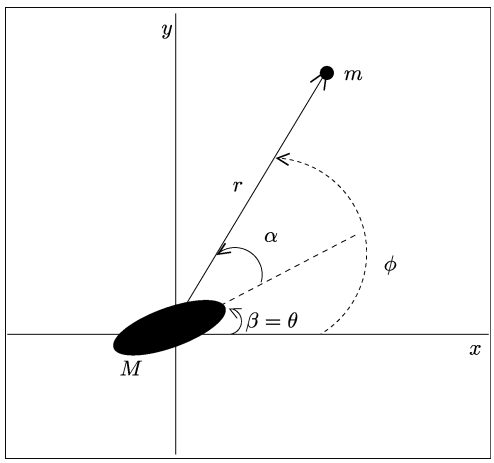

Fig. 4 Gravitational interaction of a rigid body and a sphere in the plane.

1. Reduction of the Translational Symmetry

Relative to a given inertial reference frame, the kinetic energy of the system is

$$K = \tfrac{1}{2}m\|\dot{\boldsymbol{r}}\|^2 + \tfrac{1}{2}M\|\dot{\boldsymbol{R}}\|^2 + \tfrac{1}{2}I_{zz}\dot{\theta}^2$$

where $\boldsymbol{r}$ and $\boldsymbol{R}$ are the positions of the sphere's center and the barycenter of the rigid body and the angle θ is as shown in Fig. 4.

We perform a first reduction using the invariance of the system under translations by using the fact that at the system's center of mass, $m\boldsymbol{r} + M\boldsymbol{R} = 0$. Defining $\boldsymbol{q} = \boldsymbol{r} - \boldsymbol{R}$, which is the relative position of the sphere with respect to the rigid body, one gets $\boldsymbol{r} = [M/(m+M)]\boldsymbol{q}$ and $\boldsymbol{R} = [-m/(m+M)]\boldsymbol{q}$, and the kinetic energy can be rewritten as

$$K = \tfrac{1}{2}[mM/(m+M)]\|\dot{\boldsymbol{q}}\|^2 + \tfrac{1}{2}I_{zz}\dot{\theta}^2$$

If the unit of mass is defined such that $mM/(m+M) = 1$, the unit of length is taken to be the longest axis of inertia of the rigid body, and the unit of time is chosen such that $G(m+M) = 1$, then the kinetic energy can be simplified as

$$K = \tfrac{1}{2}\|\dot{\boldsymbol{q}}\|^2 + \tfrac{1}{2}I_{zz}\dot{\theta}^2$$

The configuration space of this reduced system is the planar Euclidean group $SE(2)$, and its Lagrangian can be written locally as

$$L(\boldsymbol{q}, \theta, \dot{\boldsymbol{q}}, \dot{\theta}) = \tfrac{1}{2}\|\dot{\boldsymbol{q}}\|^2 + \tfrac{1}{2}I_{zz}\dot{\theta}^2 - V(\boldsymbol{q}, \theta) \tag{1}$$

From the Lagrangian, we obtain the momenta conjugate to the variables $(\boldsymbol{q}, \theta)$ via the Legendre transformation: $\boldsymbol{p} = \partial L/\partial\dot{\boldsymbol{q}} = \dot{\boldsymbol{q}}$, $p_\theta = \partial L/\partial\dot{\theta} = I_{zz}\dot{\theta}$. Thus, its corresponding Hamiltonian is

$$H = \tfrac{1}{2}\|\boldsymbol{p}\|^2 + (1/2I_{zz})p_\theta^2 + V(\boldsymbol{q}, \theta) \tag{2}$$

This system still has an overall rotational symmetry.

2. Reduction of the Rotational Symmetry

We first perform two preliminary (canonical) changes of variables that will simplify the action of the symmetry group $SO(2) = S^1$ on the configuration space $SE(2)$. The first change is the introduction of polar coordinates:

$$q_x = r\cos\phi, \qquad p_x = p_r\cos\phi - (p_\phi/r)\sin\phi$$

$$q_y = r\sin\phi, \qquad p_y = p_r\sin\phi + (p_\phi/r)\cos\phi$$

The second one is the use of the relative angles

$$\alpha = \phi - \theta, \qquad p_\alpha = p_\phi$$

$$\beta = \theta, \qquad p_\beta = p_\phi + p_\theta$$

as shown in Fig. 4. These changes are the first steps in rewriting the equations of the system using the body frame of the rigid body. The Lagrangian becomes[17]

$$L = \tfrac{1}{2}\dot{r}^2 + \tfrac{1}{2}r^2\dot{\alpha}^2 + \tfrac{1}{2}\left(r^2 + I_{zz}\right)\dot{\beta}^2 + r^2\dot{\alpha}\dot{\beta} - V(r, \alpha)$$

Note that the potential does not depend on the orientation angle θ because of its invariance under rotations. Also the action of the symmetry group $SO(2)$ on the (r, α, β) variables is trivial:

$$\Phi_\varphi(r, \alpha, \beta) = (r, \alpha, \beta + \varphi)$$

The Hamiltonian in these new coordinates is given by

$$H = \tfrac{1}{2}p_r^2 + \left(1/2r^2 + 1/2I_{zz}\right)p_\alpha^2 + (1/2I_{zz})p_\beta^2 - (1/I_{zz})p_\alpha p_\beta + V(r, \alpha) \tag{3}$$

where $p_\alpha = r^2\dot{\alpha} + r^2\dot{\beta}$ and $p_\beta = r^2\dot{\alpha} + (r^2 + I_{zz})\dot{\beta}$. Notice that β is a cyclic variable of the Hamiltonian (3), and therefore its conjugate momentum p_β is conserved.

To perform the reduction of the Hamiltonian, we apply cotangent bundle reduction theory (for details, see Refs. 15 and 16). The momentum map is given by

$$\boldsymbol{J}(r, \alpha, \beta, p_r, p_\alpha, p_\beta) = p_\beta$$

which corresponds to the angular momentum of the system in the new coordinates. The locked inertia tensor is $\mathbb{I}(r, \alpha, \beta) = r^2 + I_{zz}$, which is the instantaneous inertia tensor when the relative motion of the two body is locked. The mechanical connection is the 1-form given by

$$\mathcal{A}(r, \alpha, \beta) = \left[r^2/\left(r^2 + I_{zz}\right)\right]\mathrm{d}\alpha + \mathrm{d}\beta$$

For a fixed $p_\beta = \gamma$, we can perform the momentum shift from $\boldsymbol{J}^{-1}(\gamma)$ to $\boldsymbol{J}^{-1}(0)$ by means of

$$\tilde{p}_r = p_r, \qquad \tilde{p}_\alpha = p_\alpha - \left[\gamma r^2/\left(r^2 + I_{zz}\right)\right], \qquad \tilde{p}_\beta = 0$$

The reduced Hamiltonian in $\boldsymbol{J}^{-1}(0)/S^1$ has only two degrees of freedom

$$H = \tfrac{1}{2}\tilde{p}_r^2 + \tfrac{1}{2}\left(1/r^2 + 1/I_{zz}\right)\tilde{p}_\alpha^2 + V(r, \alpha) + \gamma^2/2\left(r^2 + I_{zz}\right) \tag{4}$$

with the noncanonical reduced symplectic form given by

$$\omega_\gamma = \mathrm{d}r \wedge \mathrm{d}\tilde{p}_r + \mathrm{d}\alpha \wedge \mathrm{d}\tilde{p}_\alpha - \frac{2\gamma I_{zz}r}{(r^2 + I_{zz})^2}\,\mathrm{d}r \wedge \mathrm{d}\alpha \tag{5}$$

Finally, the reduced Hamiltonian equations can be easily derived from the Hamiltonian (4) and the symplectic form (5). It is a system with two degrees of freedom, which describes the motion of the sphere in the body frame of the rigid body

$$\dot{r} = \tilde{p}_r$$

$$\dot{\alpha} = \left(\frac{1}{r^2} + \frac{1}{I_{zz}}\right)\tilde{p}_\alpha$$

$$\dot{\tilde{p}}_r = \frac{\tilde{p}_\alpha^2}{r^3} - \frac{\partial V\left(r, \alpha\right)}{\partial r} + \frac{\gamma^2 r}{\left(r^2 + I_{zz}\right)^2} + \frac{2\gamma I_{zz}r}{\left(r^2 + I_{zz}\right)^2}\left(\frac{1}{r^2} + \frac{1}{I_{zz}}\right)\tilde{p}_\alpha$$

$$\dot{\tilde{p}}_\alpha = -\frac{\partial V(r, \alpha)}{\partial \alpha} - \frac{2\gamma I_{zz}r}{\left(r^2 + I_{zz}\right)^2}\tilde{p}_r$$

where $V(r, \alpha)$ is the potential of the rigid body in the body frame.

3. Simple Potential of the Rigid Body

For simplicity, we approximate the potential of the rigid body by the gravitational potential of three masses attached with two massless rigid rods. The two external masses are assumed to be identical (see Fig. 5). Similarly, a recent related paper[18] treats the mutual dynamics of a sphere and a two-mass body but in a slightly different context.

Following the results obtained in the last section, the Hamiltonian with this potential is

$$H = \frac{1}{2}\tilde{p}_r^2 + \frac{1}{2}\left(\frac{r^2 + I_{zz}}{r^2 I_{zz}}\right)\tilde{p}_\alpha^2 + V_\gamma(r, \alpha) \tag{6}$$

where

$$V_\gamma = -\frac{1 - 2\mu}{r} - \mu\left(\frac{1}{r_u} + \frac{1}{r_d}\right) + \frac{\gamma^2}{2\left(r^2 + I_{zz}\right)}$$

Here (see Fig. 5), $\gamma \in \mathbb{R}$, $\mu = m_s/(m_b + 2m_s)$, $\nu = m/(m+M)$, $r_u^2 = r^2 + 2\,\mathrm{d}r\cos\alpha + \mathrm{d}^2$, and $r_d^2 = r^2 - 2\,\mathrm{d}r\cos\alpha + d^2$. The moment of inertia of the system is $I_{zz} = \mu/2\nu$. Sometimes it will be useful to use I_{zz} as a parameter instead of ν. The Hamiltonian equations can be readily derived from Hamiltonian (6) and the symplectic form (5).

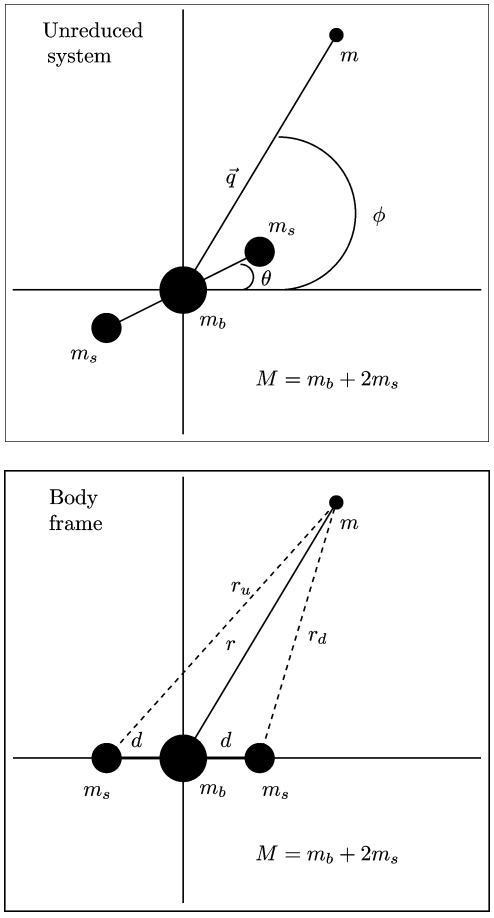

Fig. 5 Simple model for the potential of the rigid body.

B. Relative Equilibria for the Binary

The relative equilibria of the asteroid pair in the reduced system can be obtained from the Hamiltonian (6). They satisfy the following equations:

$$\tilde{p}_r = \tilde{p}_\alpha = 0, \qquad \frac{\partial V_\gamma}{\partial r} = \frac{\partial V_\gamma}{\partial \alpha} = 0$$

After some computations, we obtain

$$p_r = 0, \qquad p_\alpha = \frac{\gamma r^2}{r^2 + I_{zz}}, \qquad \mu \, \mathrm{d} r \sin\alpha \left(\frac{1}{r_d^3} - \frac{1}{r_u^3} \right) = 0$$

$$\frac{1 - 2\mu}{r^2} - \frac{\gamma^2 r}{(r^2 + I_{zz})^2} + \mu \left(\frac{r + \mathrm{d}\cos\alpha}{r_u^3} - \frac{r - \mathrm{d}\cos\alpha}{r_d^3} \right) = 0$$

The third equation gives us the solution for the orientation angle α and the last one the distance r. From the first two equations, we can compute the momenta once the relative positions are known. There are two types of solutions, depending on the value of the orientation angle: 1) collinear configurations, with $\sin\alpha = 0$, $\alpha \in \{0, \pi\}$; and 2) T configurations, with $r_d = r_u$, which is equivalent to $\alpha = \pm\pi/2$.

1. *Stability of the Relative Equilibria*

We do not perform a general study of the stability of these relative equilibria. Instead, we will focus only on the cases when the rigid body is "big" ($\nu \ll 1$) and when the binary is in a stable configuration, which enables us to study the motion of a spacecraft near the pair. Our numerical experiments show that the collinear configurations are likely to be unstable (see Ref. 12 for a related problem). These results motivate one to study the T configuration in more detail. By computing the eigenvalues of the linearized vector field at the relative equilibria for a range of parameter values, we can establish the spectral stability of these relative equilibria as parameter values vary.

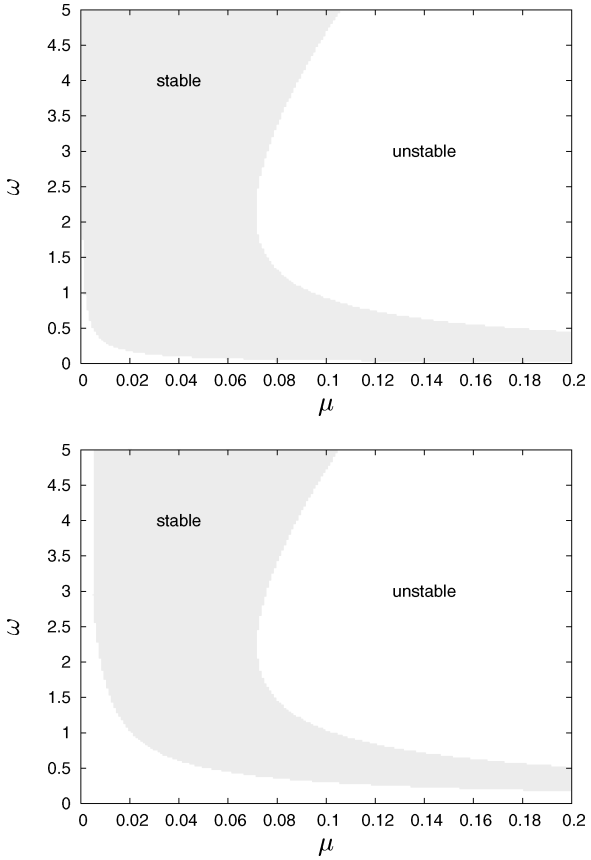

Fig. 6 Spectral stability of the T configuration (gray zone): top, $\nu = 10^{-3}$; and bottom; $\nu = 10^{-2}$.

An example of the results is shown in Fig. 6. Here, we have fixed the relative mass of the binary ν to two typical values[13]: $\nu = 10^{-2}$ and 10^{-3}. For instance, the mass parameter for some known binaries are $\nu \simeq 10^{-4}$ for Ida, $\nu \simeq 10^{-3}$ for Kalliope, $\nu \simeq 2 \times 10^{-3}$ for Eugenia, $\nu \simeq 2 \times 10^{-2}$ for Dionysus, and $\nu \simeq 5 \times 10^{-2}$ for 2000 DP107.

In Fig. 6, the parameter values corresponding to spectrally stable relative equilibria are colored in gray. The values of the parameters studied here are $\mu \in (0, 0.2)$ and $\omega \equiv (\gamma / I_{zz}) \in (0, 5)$. The moment of inertia of the rigid body is taken as $I_{zz} = \mu/\nu$.

In Sec. III, we use the result summarized in Fig. 6 to choose concrete values for the parameters such that the T configuration is spectrally stable.

2. *Reconstruction of the Relative Equilibria*

Because we are interested in visualizing the relative equilibria in the initial configuration space, we need to reconstruct the dynamics from the reduced coordinates. In our case, it is not difficult to see that the reconstruction equations for the group variables are given by

$$\dot{\theta} = p_\theta / I_{zz}, \qquad p_\theta = \gamma - p_\alpha \tag{7}$$

If a solution in the reduced space $[r(t), \alpha(t), p_r(t), p_\alpha(t)]$ is known, one can integrate Eq. (7) to obtain the evolution of the orientation angle of the rigid body $\theta(t)$.

For instance, if the reduced system is in one of the relative equilibria just described, the conjugate momenta of the orientation angle variable is constant, that is, $p_\theta = \text{constant}$, and the equation for the attitude (7) is trivial to integrate

$$\dot{\theta} = \frac{p_\theta}{I_{zz}} \equiv \omega_L \qquad \text{which implies that} \qquad \theta = \omega_L t + \theta_0$$

Hence, in the unreduced system the relative equilibria are periodic orbits of period $T_L = 2\pi/\omega_L$. For example, for one of the

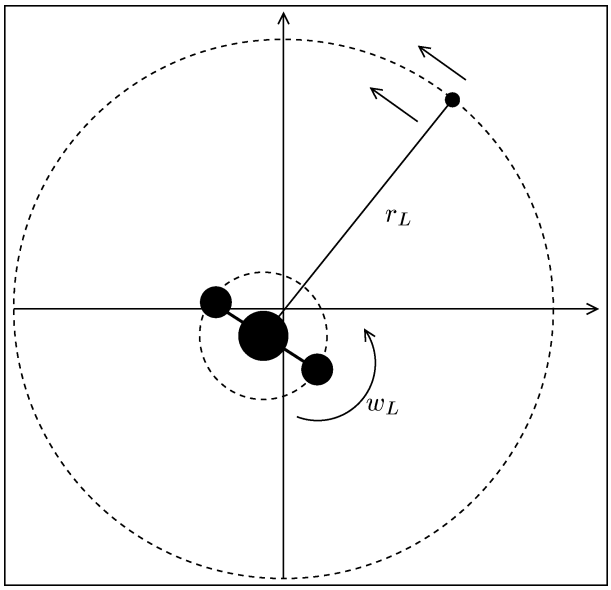

Fig. 7 Relative equilibria for the T configuration visualized in the unreduced reference frame. The system is rotating uniformly with angular velocity ω_L.

T configuration points ($r \equiv r_L$, $\alpha = \pi/2$) the solution for a rigid body and a sphere is a T-shaped object, which is rotating uniformly at rate ω_L (see Fig. 7).

III. Models for the Motion of the Spacecraft

In this section, we construct two models for the motion of a spacecraft near the asteroid pair. We assume that the binary is in a specific relative equilibrium with $\alpha = \pi/2$ and the system is rotating uniformly with frequency ω_L, as in Fig. 7. In the first model, we assume that the motion of the spacecraft is affected only by the gravitational interaction of the asteroid pair. In the second model, we add the effect of the perturbation of the sun on the equations of motion of the spacecraft.

A. Basic T Model

Suppose that $\boldsymbol{Q}_0$ and $\{\boldsymbol{Q}_u, \boldsymbol{Q}_d\}$ are, respectively, the position vectors of the central and the two external masses of the rigid body in an inertial reference frame centered at the system's barycenter. Let us also call $\boldsymbol{Q}_s$ the position of the sphere and $\boldsymbol{Q}$ the position of the spacecraft in the same frame.

In this inertial reference frame, the kinetic energy of the spacecraft is given by $K = \frac{1}{2}\|\dot{\boldsymbol{Q}}\|^2$, and thus the corresponding momenta can be defined as $\boldsymbol{P} = \dot{\boldsymbol{Q}}$. The equations of motion for the spacecraft can be written as

$$\dot{\boldsymbol{Q}} = \boldsymbol{P}, \qquad \dot{\boldsymbol{P}} = -\frac{\partial V}{\partial \boldsymbol{Q}}$$

where the potential is given by

$$V = -G\left(\frac{m_b}{\|\boldsymbol{Q}_{0p}\|} + \frac{m_s}{\|\boldsymbol{Q}_{\mathrm{up}}\|} + \frac{m_s}{\|\boldsymbol{Q}_{\mathrm{dp}}\|} + \frac{m}{\|\boldsymbol{Q}_{\mathrm{sp}}\|}\right)$$

with $M = m_b + 2m_s$, $\nu = m/(m+M)$, and $\boldsymbol{Q}_{jp} = \boldsymbol{Q} - \boldsymbol{Q}_j$, for $j = 0, u, d, s$.

We now perform a rotation to fix the rigid-body's longest principal axis orthogonal to the x axis: $\boldsymbol{Q} = \mathcal{R}_{\theta_L}\boldsymbol{q}$, where $\boldsymbol{q} = (x, y, z)$ and $\mathcal{R}_{\theta_L}$ is the counterclockwise rotation of angle $\theta_L = \omega_L t + \theta_0$ in the xy plane,

$$\mathcal{R}_\theta = \begin{pmatrix} \cos\theta & -\sin\theta & 0 \\ \sin\theta & \cos\theta & 0 \\ 0 & 0 & 1 \end{pmatrix}$$

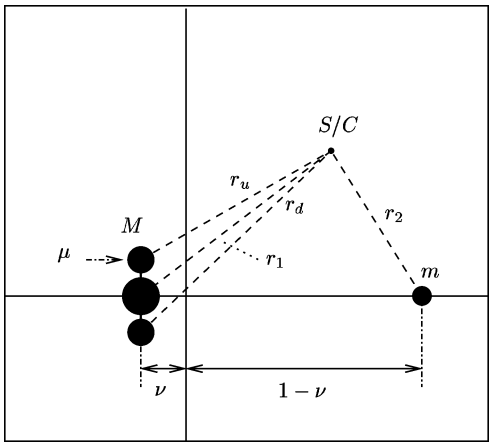

Fig. 8 Basic T model for the spacecraft (S/C).

In this rotating frame, the equations of motion for the spacecraft are

$$\dot{x} = p_x + \dot{\theta}_L y, \qquad \dot{p_x} = \dot{\theta}_L p_y - \frac{\partial V}{\partial x}$$

$$\dot{y} = p_y - \dot{\theta}_L x, \qquad \dot{p_y} = -\dot{\theta}_L p_x - \frac{\partial V}{\partial y}$$

$$\dot{z} = p_z, \qquad \dot{p_z} = -\frac{\partial V}{\partial z}$$

where

$$V = -G\left(\frac{m_b}{\|\boldsymbol{q}_{0p}\|} + \frac{m_u}{\|\boldsymbol{q}_{\mathrm{up}}\|} + \frac{m_d}{\|\boldsymbol{q}_{\mathrm{dp}}\|} + \frac{m}{\|\boldsymbol{q}_{\mathrm{sp}}\|}\right)$$

Here, $\dot{\theta_L} = \omega_L$, and $\boldsymbol{q}_{jp} = \boldsymbol{q} - \boldsymbol{q}_j$, for $j = 0, u, d, s$. Note that $\boldsymbol{q}_j$ (position vectors of the masses in the rigid-body frame) are known from the T-configuration relative equilibria: $\boldsymbol{q}_0 = (-\nu r_L, 0, 0)$, $\boldsymbol{q}_u = (-\nu r_L, 1/2, 0)$, $\boldsymbol{q}_d = (-\nu r_L, -1/2, 0)$, and $\boldsymbol{q}_s = [(1-\nu)r_L, 0, 0]$.

These equations are Hamiltonian (in a canonical way) with the following Hamiltonian function:

$$H = \tfrac{1}{2}\left(p_x^2 + p_y^2 + p_z^2\right) + \omega_L(yp_x - xp_y) + V(x, y, z)$$

Let us redefine nondimensional units for the spacecraft model as follows: take the new unit of length to be the distance between the center of masses of the rigid body and the sphere, the unit of time to be such that $\omega_L = 1$, so that the asteroid pair does a complete revolution in 2π units of time, and the unit of mass such that $GmM = 1$.

Then, the Hamiltonian for the motion of the spacecraft can be written as an $\mathcal{O}(\mu)$ perturbation of the RTBP with mass-ratio ν

$$H = \tfrac{1}{2}\left(p_x^2 + p_y^2 + p_z^2\right) + (yp_x - xp_y) + V(x, y, z) \qquad (8)$$

where

$$V = -(1-\nu)(1-2\mu)/r_1 - \nu/r_2 - \mu(1-\nu)(1/r_u + 1/r_d)$$

Here, $r_1^2 = (x+\nu)^2 + y^2 + z^2$, $r_2^2 = [x-(1-\nu)]^2 + y^2 + z^2$, $r_u^2 = (x+\nu)^2 + (y-d)^2 + z^2$, $r_d^2 = (x+\nu)^2 + (y+d)^2 + z^2$, and $d = 1/2r_L$, as in Fig. 8.

B. T Model: Perturbation of the Sun

We now take into consideration the direct effect of sun's perturbation on the spacecraft. We assume, as a first approximation, that the uniform rotation of the binary is not affected by the sun and that the center of masses of the binary is also rotating uniformly around the sun with a rate denoted by ω_s, as in Fig. 9. This idea is similar to the construction of the well-known bicircular problem[19] that has been used to model some restricted four-body problems in the solar system.[20,21]

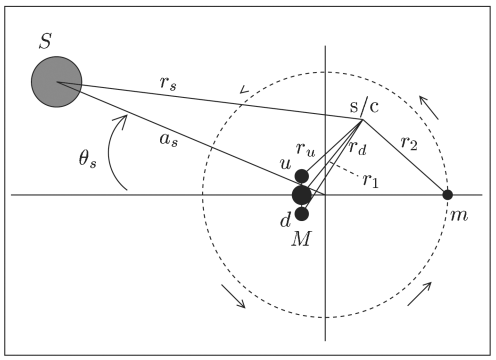

Fig. 9 Perturbation of the sun on the T model.

We start in inertial coordinates, where we denote $\boldsymbol{Q}$ as the position vector of the spacecraft measured from the sun and $\{\boldsymbol{Q}_1, \boldsymbol{Q}_u, \boldsymbol{Q}_d, \boldsymbol{Q}_2\}$ the ones corresponding, respectively, to the center, upper, and lower mass of the rigid body and to the sphere. In these coordinates, the equations of motion for the spacecraft are

$$\ddot{\boldsymbol{Q}} = -\frac{\partial V}{\partial \boldsymbol{Q}}$$

where the Newtonian potential is

$$V = -\frac{m_1}{\|\boldsymbol{Q}-\boldsymbol{Q}_1\|} - \frac{m_u}{\|\boldsymbol{Q}-\boldsymbol{Q}_u\|} - \frac{m_d}{\|\boldsymbol{Q}-\boldsymbol{Q}_d\|} - \frac{m_2}{\|\boldsymbol{Q}-\boldsymbol{Q}_2\|} - \frac{m_s}{\|\boldsymbol{Q}\|}$$

We perform two changes of variables to write the equations in the so-called synodical coordinates relative to the binary. The first one is a translation from the sun to the center of masses of the asteroid pair: $\boldsymbol{Q} = \boldsymbol{Q}_{\mathrm{CM}_T} + \boldsymbol{R}$, where $\boldsymbol{Q}_{\mathrm{CM}_T} = (a_s \cos\bar{\theta}_s, a_s \sin\bar{\theta}_s, 0)$, $\bar{\theta}_s = n_s t + \bar{\theta}_s^0$, and $\boldsymbol{R} = (X, Y, Z)$ is the position of the spacecraft from the center of masses of the T model (CM_T). After this (time-dependent) translation, the equations for the spacecraft are

$$\ddot{\boldsymbol{R}} = a_s n_s^2 (\cos n_s t, \sin n_s t, 0) - \frac{\partial V}{\partial \boldsymbol{R}}$$

The second change of variables is a (time-dependent) rotation that fixes the binary to the x axis:

$$X = x\cos t - y\sin t, \qquad Y = x\sin t + y\cos t, \qquad Z = z$$

From here, write

$$\ddot{x} - 2\dot{y} - x = \ddot{X}\cos t + \ddot{Y}\sin t$$

$$\ddot{y} + 2\dot{x} - y = \ddot{Y}\cos t - \ddot{X}\sin t$$

Recall that, in the relative equilibria of the binary, $(X_1, Y_1) = (-\nu\cos t, -\nu\sin t)$, $(X_2, Y_2) = [(1-\nu)\cos t, (1-\nu)\sin t]$, and similar expressions for m_u and m_d hold. If we denote $\boldsymbol{r} = (x, y, z)$ to be the position of the spacecraft in these rotating coordinates, we obtain

$$\ddot{x} = 2\dot{y} + x + \frac{m_s}{a_s^2}\cos\theta_s - m_1\frac{x+\nu}{\|\boldsymbol{r}-\boldsymbol{r}_1\|} - m_2\frac{x-(1-\nu)}{\|\boldsymbol{r}-\boldsymbol{r}_2\|}$$
$$- m_u\frac{x+\nu}{\|\boldsymbol{r}-\boldsymbol{r}_u\|} - m_d\frac{x+\nu}{\|\boldsymbol{r}-\boldsymbol{r}_d\|} - m_s\frac{x+a_s\cos\theta_s}{\|\boldsymbol{r}-\boldsymbol{r}_s\|}$$

$$\ddot{y} = -2\dot{x} + y - \frac{m_s}{a_s^2}\sin\theta_s - m_1\frac{y}{\|\boldsymbol{r}-\boldsymbol{r}_1\|} - m_2\frac{y}{\|\boldsymbol{r}-\boldsymbol{r}_2\|}$$
$$- m_u\frac{y-d}{\|\boldsymbol{r}-\boldsymbol{r}_u\|} - m_d\frac{y+d}{\|\boldsymbol{r}-\boldsymbol{r}_d\|} - m_s\frac{y-a_s\sin\theta_s}{\|\boldsymbol{r}-\boldsymbol{r}_s\|}$$

$$\ddot{z} = -m_1\frac{z}{\|\boldsymbol{r}-\boldsymbol{r}_1\|} - m_2\frac{z}{\|\boldsymbol{r}-\boldsymbol{r}_2\|} - m_u\frac{z}{\|\boldsymbol{r}-\boldsymbol{r}_u\|}$$
$$- m_d\frac{z}{\|\boldsymbol{r}-\boldsymbol{r}_d\|} - m_s\frac{z}{\|\boldsymbol{r}-\boldsymbol{r}_s\|}$$

where $\theta_s = t - \bar{\theta}_s = t - n_s t - \pi$ and the third Kepler law has been used in the computations.

Finally, defining the momenta in the usual way via the Legendre transform, we get

$$\dot{x} = p_x + y, \qquad \dot{y} = p_y - x, \qquad \dot{z} = p_z$$

the equations of motion are Hamiltonian, and the Hamiltonian function can be written as a periodic perturbation of the T model:

$$H = \tfrac{1}{2}\left(p_x^2 + p_y^2 + p_z^2\right) + (yp_x - xp_y)$$
$$- \left(m_s \big/ a_s^2\right)(x\cos\theta_s - y\sin\theta_s) + V(x, y, z, \theta_s) \tag{9}$$

where

$$V = -\frac{(1-\nu)(1-2\mu)}{r_1} - \frac{\nu}{r_2} - \mu(1-\nu)\left(\frac{1}{r_u} + \frac{1}{r_d}\right) - \frac{m_s}{r_s} \tag{10}$$

Here, $r_s^2 = (x + a_s\cos\theta_s)^2 + (y - a_s\sin\theta_s)^2 + z^2$ and $\theta_s = \omega_s t + \theta_s^0$.

IV. Nonlinear Dynamics near the Perturbed Lagrange Points

Recall that the triangular libration points of the RTBP are spectrally stable if the mass parameter is smaller than the Routh critical value. In this case, the nonlinear dynamics around these points can be studied by means of normal form techniques.[14,22,23] In this section, we study the effect of the rigid body and the sun near the triangular points and use similar techniques to describe the nonlinear dynamics near them. The normal form expansion of the Hamiltonian at the equilibrium points provides a way to obtain all possible motions in a vicinity of these points. Hence, this procedure enables us to find many quasi-periodic trajectories near the triangular points that can be used for the spacecraft to orbit around the asteroid pair. The advantage of having a symbolic representation of the Hamiltonian is that it allows the prescribing of the initial conditions for these quasi-periodic motions very easily.

To choose the parameters for the models developed in Sec.III, we use the stability results of the asteroid pair relative equilibria described in Sec II.B. In particular, we choose the parameters such that the binary is in a stable T configuration. The mass ratio between the sphere and the rigid body is taken as a typical value for certain type of binaries, $\nu = m/(m+M) = 0.001$. The grade of mass dispersion μ of the rigid body is chosen to be relatively small, $\mu = 0.02$, and its moment of inertia is taken as $I_{zz} = 20$. The angular momentum is also taken to be moderately small, $\gamma = 4$, so that the T configuration is spectrally stable with $\omega = 0.2$ as its corresponding frequency (see Fig .6). With these parameters, the T-configuration solution is found at $r_L = 5.07830172847938$ times the largest dimension of the rigid body. Also, the selection of these particular values ensures that the perturbed triangular points will be spectrally stable.

When including the perturbation of the sun, we assume that the binary is in the main asteroid belt ($a_s \approx 3$ astronomical unit) and that its total mass is that of a medium/large-size asteroid (10^{17} kg). This gives us the remaining parameters for the second model in nondimensional units: $a_s = 1.5 \times 10^6$ and $m_s = 10^{13}$. The relative frequency of the sun ω_s can be easily obtained from the third Kepler law: $\omega_s = 0.998278674068352$.

Using these parameter values to make the actual computations, we perform a local study of the nonlinear dynamics for the spacecraft near the Lagrangian stable regions, knowing that the qualitative results will be valid for a wide range of parameters.

The implicit function theorem shows that, if the perturbations are small and are under some non-resonance conditions, the RTBP triangular points persist in the basic T model and are replaced by stable periodic orbits after taking into consideration of the sun's perturbation (see Fig. 10).

We focus on the L_4 case, although the same results can be obtained for L_5. The new fixed point that plays the role of L_4 in the T model will be called L_4', and the periodic orbit that has the same period as the sun's perturbation $T_s = 2\pi/w_s$ will be named $PO(L_4')$.

Table 1 Normal frequencies for the linear oscillators around the elliptic fixed point L_4' and periodic orbit $PO(L_4')$

Normal mode	L_4'	$PO(L_4')$
ω_1	−0.10702011607983	−0.10702058242758
ω_2	0.99366842989866	0.99366615570514
ω_3	1.00058470215019	1.00058692342681

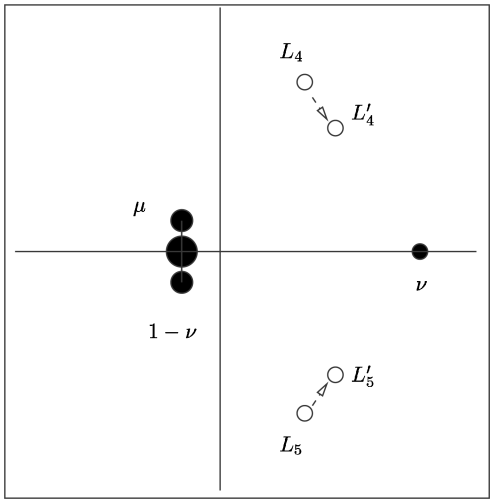

Fig. 10 Schematic diagram showing the triangular equilibria of the RTBP persist when one of the primaries is not a point mass but an extended rigid body.

A. Study of the Dynamics at L_4' and $PO(L_4')$

Here we compute the eigenvalues of the linearized vector field at L_4' or the Floquet multipliers of the periodic orbit $PO(L_4')$. For the example, they correspond to elliptic objects and are displayed in Table 1.

Thus, the T-model system is elliptic at L_4' and around $PO(L_4')$, and we can study the nonlinear dynamics around these objects by constructing a high-order normal form around the fixed point L_4' and around the periodic orbit $PO(L_4')$.

This normal form computation allows us to extend the study of the dynamics in a neighborhood of the elliptic invariant objects (fixed point and periodic orbit) and provides a way to integrate the equations of motion in this neighborhood. Once the complete nonlinear dynamics are understood, we can use this normal form to prescribe the trajectories of the spacecraft near the invariant object.

1. *Quadratic Normal Form*

We focus on the time-periodic case (for the autonomous system, the quadratic normal form corresponds to the real Jordan form of the linear differential equations): After having moved the origin to the periodic orbit $PO(L_4')$ (this translation is T_s periodic), the linear part of the vector field is of the form $\dot{u} = L(t)u$, where $L(t)$ is a 6×6 T_s-periodic real matrix.

The Floquet theorem ensures the existence of a linear T_s-periodic change of variables $v = C(t)u$ such that the linear part of the vector field reduces to a linear system with constant coefficients $\dot{v} = \Lambda v$, where Λ is a 6×6 real constant matrix.

It is possible[4] to choose the change of variables such that $C(t)$ is symplectic (the method requires this condition because the changes are made directly on the Hamiltonian function) and the matrix Λ takes the form

$$\Lambda = \left(\begin{array}{c|c} 0_3 & \Omega \\ \hline -\Omega & 0_3 \end{array}\right)$$

where 0_3 is the 3×3 zero matrix and $\Omega = \mathrm{diag}(\omega_1, \omega_2, \omega_3)$ is the diagonal matrix containing the frequencies w_j corresponding to the three normal modes of the periodic orbit [recall that the periodic orbit $PO(L_4')$ is elliptic].

Implementing these changes of variables, the normal form up to degree 2 only contains monomials of order 2. The order 0 is irrelevant in the equations of motion, and the order 1 terms are eliminated because the origin is a fixed point after the translation. So, the normal form up to degree two is a quadratic form given by

$$H_2 = \omega_1\left[\left(x_1^2 + y_1^2\right)/2\right] + \omega_2\left[\left(x_2^2 + y_2^2\right)/2\right] + \omega_3\left[\left(x_3^2 + y_2^3\right)/2\right]$$

Finally, it is convenient, before starting the high-order normal form, to express the variables in complex notation

$$x_j = (q_j + ip_j)/\sqrt{2}, \qquad y_j = (iq_j + p_j)/\sqrt{2}, \qquad j = 1, 2, 3$$

which rewrites the quadratic part of the Hamiltonian in the following form:

$$H_2 = i\omega_1 q_1 p_1 + i\omega_2 q_2 p_2 + i\omega_3 q_3 p_3$$

where the values for the frequencies w_j can be found in Table 1.

2. *High-Order Normal Form*

Prior to the construction of the high-order normal form, we expand the Hamiltonian in Fourier–Taylor series (Taylor series in the autonomous case) and insert the previous linear changes to this expansion to obtain

$$H = i\omega_1 q_1 p_1 + i\omega_2 q_2 p_2 + i\omega_3 q_3 p_3 + \sum_{j \geq 3} H_j(q, p, \theta_s)$$

which will be the starting input object of the following construction. For details on how to expand the current type of potential functions, see Ref. 4.

To build the normal form of order higher than 2, we use the Lie series method (see Ref. 24, for an introduction) implemented as in Ref. 14. We use a hand-made software that contains symbolic algebra routines that deal with the Taylor and Fourier–Taylor series appearing in the computations. We sketch one step of the process for the time-periodic case. For the autonomous case, skip the dependence with time.

Let us assume that the Hamiltonian is already in normal form up to degree $r-1$:

$$H = \omega_s p_{\theta_s} + H_2^{(n)}(qp) + \sum_{j=4, j=\dot{2}}^{r-1} H_j^{(n)}(qp) + H_r(q, p, \theta_s) + H_{r+1}(q, p, \theta_s) + \cdots$$

where $H_r(q, p, \theta_s) = \sum_{|k|=r} h_r^k(\theta_s) q^{k^1} p^{k^2}$, $\theta_s = \omega_s t + \theta_0$, and $k = (k^1, k^2) \in \mathbb{Z}^3 \times \mathbb{Z}^3$. The extra term $\omega_s p_{\theta_s}$ has been introduced to make the Hamiltonian autonomous, and p_{θ_s} is the conjugate momenta to the θ_s variable.

We are interested in making a change of variables such that the homogeneous polynomial $H_r(q, p, \theta_s)$ takes a form that is as simple as possible. In particular, we want this change to make the monomials contained in it autonomous. The canonical change given by the following generating function satisfies these requirements:

$$G_r = G_r(q, p, \theta_s) = \sum_{\substack{|k|=r \\ k^1 \neq k^2}} \frac{-h_r^k(\theta_s)}{\langle \omega, k^2 - k^1 \rangle} q^{k^1} p^{k^2}$$

where $\langle , \rangle$ denotes the dot product.

The new Hamiltonian obtained with this change of variables is obtained with the Lie series[24]:

$$H' = H + \{H, G_r\} + \tfrac{1}{2!}\{\{H, G_r\}, G_r\} + \tfrac{1}{3!}\{\{\{H, G_r\}, G_r\}, G_r\} + \cdots$$

and can be written as

$$H' = \omega_s p_{\theta_s} + H_2^{(n)}(qp) + \sum_{j=4, j=\dot{2}}^{r-1} H_j^{(n)}(qp) + H_r^{(n)}(qp) + H'_{r+1}(q, p, \theta_s) + \cdots$$

Table 2 Coefficients of the normal forms up to order 3 in the actions

k_1[a]	k_2[a]	k_3[a]	h_k(T model)[b]	h_k(T model + sun)[c]
1	0	0	−1.07020116079827*e*−01	−1.07020582427575*e*−01
0	1	0	9.93668429898665*e*−01	9.93666155705138*e*−01
0	0	1	1.00058470215019*e*+00	1.00058692342681*e*+00
2	0	0	1.98209282337547*e*+00	1.98210606475071*e*+00
1	1	0	−8.41335633534186*e*−02	−8.41363103519259*e*−02
0	2	0	3.34451789294228*e*−02	3.34473273382156*e*−02
1	0	1	9.77435542208162*e*−02	9.77447151079432*e*−02
0	1	1	1.62579166640980*e*−02	1.62670378418912*e*−02
0	0	2	−7.22623320607685*e*−04	−7.23728487410444*e*−04
3	0	0	7.23164870868422*e*+01	7.23172271456241*e*+01
2	1	0	2.40637121303353*e*+01	2.40641088603377*e*+01
1	2	0	6.06695219686117*e*+00	6.06715074575221*e*+00
0	3	0	−9.09462225134519*e*−02	−9.09462282070405*e*−02
2	0	1	−3.51875180623665*e*+00	−3.51880095271078*e*+00
1	1	1	3.17368174336265*e*+00	3.17373202727457*e*+00
0	2	1	−1.72093135781978*e*−01	−1.72064978874555*e*−01
1	0	2	−1.02419399482606*e*−01	−1.02420550719694*e*−01
0	1	2	−6.60967536055335*e*−03	−6.64293506149859*e*−03
0	0	3	3.82965067009504*e*−05	3.82868741518696*e*−05

[a]The first three columns contain the exponents of the actions.
[b]The fourth column corresponds to the autonomous case.
[c]The fifth one to the time-perturbed model.

We iterate this process and perform all of the changes up to a high-order N. Specifically, we use $N = 32$ in the autonomous case and $N = 24$ in the time-periodic one. These particular choices are caused by RAM memory limitations, but they are sufficient for our purposes.

Finally, we write the Hamiltonian in action-angle variables (I, φ), by defining $I_j = iq_j p_j$, $j = 1, 2, 3$,

$$H = \mathcal{N}(I) + \mathcal{R}(I, \varphi, \theta_s), \qquad \mathcal{N}(I) = \sum_{|k|=1}^{N/2} h_k I_1^{k_1} I_2^{k_2} I_3^{k_3} \quad (11)$$

where the term $\mathcal{R}(I, \varphi, \theta_s)$ is the remaining part of the Hamiltonian that has not been transformed to normal form, and thus it still depends on the angles and time. This term is of order $N + 1$.

We now assume that the dynamics in a vicinity of L_4' and $PO(L_4')$ is given by the normal form Hamiltonian $\mathcal{N}(I)$. The error of this approximation can be estimated by bounding the remainder $\mathcal{R}(I, \varphi, \theta_s)$, which will be large if $\|I\|_2$ is large. Note that for $I = 0$, $\mathcal{R} = 0$. The symbolic computations result with certain values for the coefficients of the normal form expansion. These coefficients up to order 3 in the actions are given in Table 2.

Because the normal form depends only on actions, it is integrable. All motions in a (small) vicinity of L_4' and $PO(L_4')$ are periodic or quasi-periodic. They take place on invariant tori of dimensions 1, 2, and 3 (autonomous case) or 2, 3, and 4 (periodic case). See Figs. 11 and 12 for some examples. These invariant tori can be computed numerically because it is easy to pick the "good" initial condition from the normal form expansion (see the following).

3. *Test and Validity of the Normal Form Approximation*

We have also constructed the transformations (using the generating function written as a Fourier–Taylor expansion) that send points from the normal form space to the initial one and vice versa. These changes of variables not only provide a way to visualize the dynamics in the initial coordinates, but also they are very helpful to test the programs.

To check the accuracy of the computations, we proceed as follows[14]: First, we take a fixed value for the actions $I_1 = I_2 = I_3 = \lambda$, with λ small, transform this point back to the initial coordinates, and integrate it numerically using the vector field corresponding to Eqs. (8) and (9) during a time span T. Let us call this final point $\boldsymbol{x}(\lambda)$. Then, we use the normal form (11) to integrate (this integration is a trivial tabulation) the same initial condition ($I_j = \lambda$) in the normal form space for the same interval of time T and transform back the final point of the integration to the initial coordinates. We call now this point $\boldsymbol{x}'(\lambda)$.

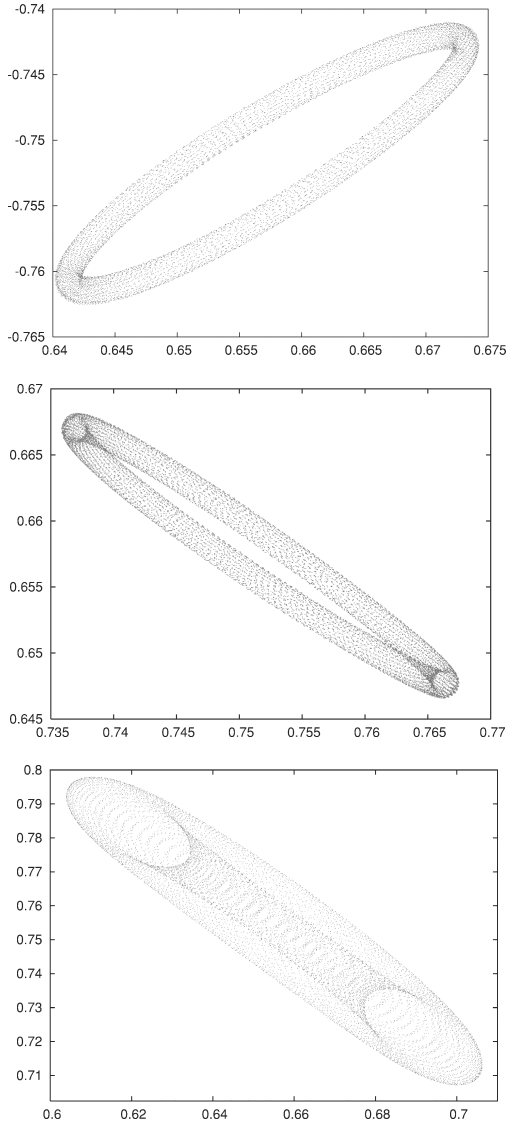

Fig. 11 Examples of stable orbits near the Lagrangian zones of the asteroid pair I: top/center, Projection into the xp_x and yp_y planes, respectively, of a three-dimensional tori bottom, Projection into the xy plane of four-dimensional tori for the time-periodic case.

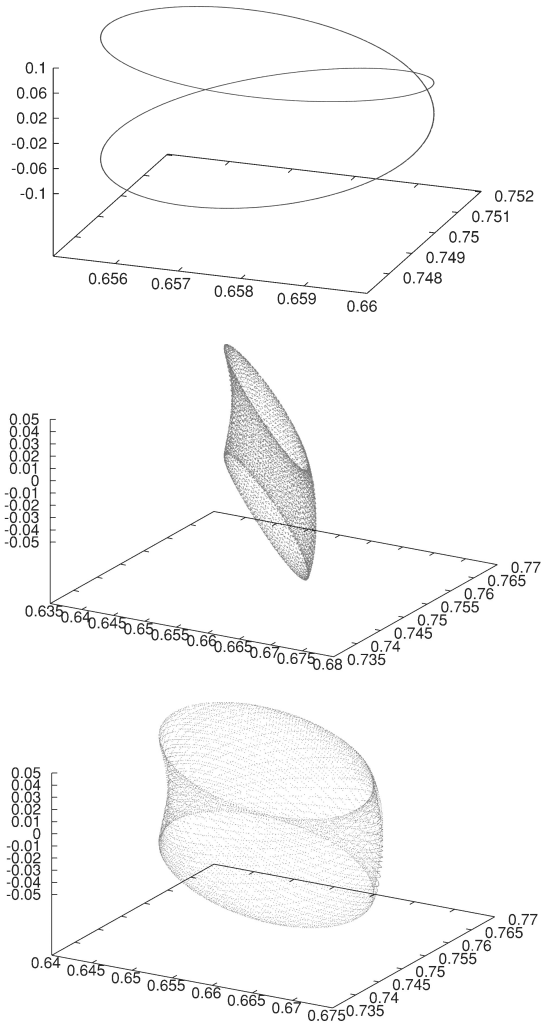

Fig. 12 Examples of stable orbits near the Lagrangian zones of the asteroid pair II: top, periodic orbit in the autonomous case; center/bottom, two examples of three-dimensional tori for the time-periodic case.

The norm of the difference between $\boldsymbol{x}(\lambda)$ and $\boldsymbol{x}'(\lambda)$ is an increasing function of λ and gives an estimation of the error that we are doing when approximating the dynamics of models (8) and (9) by the corresponding normal forms. Moreover, if we denote

$$e(\lambda) = \|\boldsymbol{x}(\lambda) - \boldsymbol{x}'(\lambda)\|_2 \tag{12}$$

the order of the error approximately behaves like

$$N \approx \frac{\ell_n[e(\lambda_1)/e(\lambda_2)]}{\ell_n(\lambda_1/\lambda_2)}$$

where N corresponds to the order of the normal form. This test is performed using different (small) values of λs and successfully passed by all our programs.

B. Spacecraft Parking Orbits

We can construct prescribed stable trajectories for the spacecraft near the elliptic objects L_4' and $PO(L_4')$ by using the dynamics given by the normal form (11). Some of these stable orbits are very interesting because we can use them to park the spacecraft to do observations of the binary as the pair orbits around the sun.

Notice that, essentially, the I_1 and I_2 actions correspond to planar motion (in the xy plane) and I_3 to the vertical direction zp_z. This observation is not exact because of the nonlinear terms, but it will be very useful for some applications.

For instance, if we are interested in performing observations of the asteroid pair with relatively high inclinations, we can prescribe

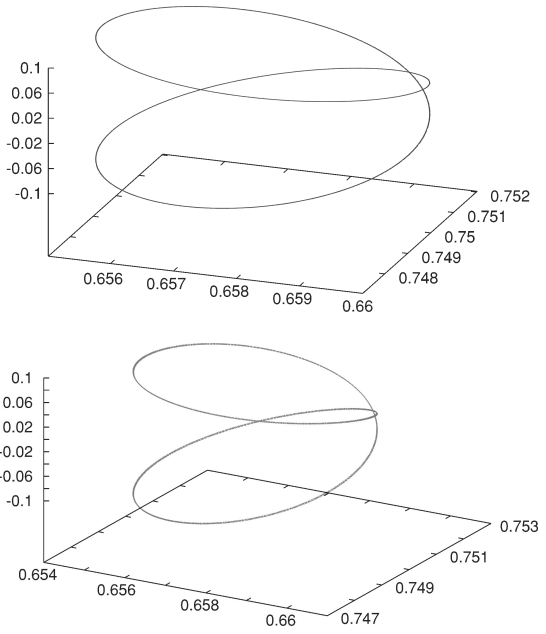

Fig. 13 Examples of relatively high inclination orbits suitable for binary observations: top, periodic orbit for the autonomous case; bottom, two-dimensional invariant torus for the time-periodic case.

values for the initial conditions with $I_1 = I_2 = 0$ and $I_3 = \lambda_3$. Then, using the nonlinear transformation that sends points from the normal form space to the initial one, we compute the point in the phase space of the T model that corresponds to this initial condition. Finally, we numerically integrate this orbit to obtain the desired invariant torus.

The concrete value of λ_3 should be taken as large as possible. This is determined by requiring that the normal form approximation error (12) is smaller than certain tolerance, $e(\lambda_3) < \text{Tol}$. In our computations, for instance, if we choose $\text{Tol} = 10^{-10}$, we can take $\lambda_3 = 0.02$. With this particular choice of actions, we obtain trajectories for the spacecraft that correspond to a periodic orbit in the autonomous case and a two-dimensional invariant torus in the time-dependent model. These particular trajectories are shown in Fig. 13. Notice that they are quite extended in the vertical direction.

V. Conclusions

We have studied simple models for the motion of a satellite about an asteroid pair, adding the effect of a nonspherical rigid body and the perturbation of the sun. We applied reduction theory for the modeling of the binary and dynamical systems methods for the study of the models. These accurate semi-analytical methods enable us to construct periodic and quasi-periodic orbits for the spacecraft very convenient for doing observations of the asteroid pair.

Even though the models studied are approximate, the results are useful at a theoretical level. The procedure used in this paper can be helpful when studying more complex models, and the qualitative dynamical behavior will persist.

In addition to make a dynamical study of the satellite motion about the binary, the paper also contributes to the study of the natural motion of the asteroid pair itself. This will play an important role when developing spacecraft missions to these bodies, a current topic of great interest.

Acknowledgments

The authors thank Daniel J. Scheeres for interesting discussions and comments. This research was partially supported by the California Institute of Technology President's Fund and NSF-ITR Grant ACI-0204932. Gabern acknowledges the support of the Fulbright–GenCat postdoctoral program, the Spanish Ministry of Science and Technology Grant BFM2003-07521-C02-01, and the Catalan Government CIRIT Grant 2001SGR–70.

References

[1]Merline, W. J., Weidenschilling, S. J., Durda, D. D., Margot, J. L., Pravec, P., and Storrs, A. D., "Asteroids Do Have Satellites," *Asteroids III*, Univ. of Arizona, Tucson, AZ, 2002, pp. 289–312.

[2]Margot, J. L., Nolan, M. C., Benner, L. A. M., Ostro, S. J., Jurgens, R. F., Giorgini, J. D., Slade, M. A., and Campbell, D. B., "Binary Asteroids in the near-Earth Object Population," *Science*, Vol. 296, No. 5572, 2002, pp. 1445–1448.

[3]Szebehely, V., *Theory of Orbits*, Academic Press, New York, 1967, pp. 20–22.

[4]Gabern, F., and Jorba, A., "A Restricted Four-Body Model for the Dynamics near the Lagrangian Points of the Sun-Jupiter System," *Discrete and Continuous Dynamical Systems—Series B*, Vol. 1, No. 2, 2001, pp. 143–182.

[5]Gabern, F., and Jorba, A., "Generalizing the Restricted Three-Body Problem. The Bianular and Tricircular Coherent Problems," *Astronomy and Astrophysics*, Vol. 420, No. 2, 2004, pp. 751–762.

[6]Scheeres, D. J., and Bellerose, J., "The Restricted Hill Full 4-Body Problem: Application to Spacecraft Motion About Binary Asteroids," *Dynamical Systems: An International Journal*, Vol. 20, No. 1, 2005, pp. 23–44.

[7]Gómez, G., Koon, W. S., Lo, M., Marsden, J. E., Masdemont, J., and Ross, S., "Connecting Orbits and Invariant Manifolds in the Spatial Restricted Three-Body Problem," *Nonlinearity*, Vol. 17, No. 5, 2004, pp. 1571–1606.

[8]Koon, W. S., Marsden, J. E., Ross, S., Lo, M., and Scheeres, D., "Geometric Mechanics and the Dynamics of Asteroid Pairs," *Annals of the New York Academy of Sciences*, Vol. 1017, May 2004, pp. 11–38.

[9]Maciejewski, A. J., "Reduction, Relative Equilibria and Potential in the Two Rigid Bodies Problem," *Celestial Mechanics and Dynamical Astronomy*, Vol. 63, No. 1, 1996, pp. 1–28.

[10]Scheeres, D. J., "Stability in the Full Two-Body Problem," *Celestial Mechanics and Dynamical Astronomy*, Vol. 83, No. 1–4, May 2002, pp. 155–169.

[11]Scheeres, D. J., "Stability of Binary Asteroids," *Icarus*, Vol. 159, No. 2, 2002, pp. 271–283.

[12]Scheeres, D. J., "Stability of Relative Equilibria in the Full Two-Body Problem," *Annals of the New York Academy of Science*, Vol. 1017, May 2004, pp. 81–94.

[13]Scheeres, D. J., and Augenstein, S., "Spacecraft Motion About Binary Asteroids," AAS/AIAA Paper 03-564, Astrodynamics Specialist Conferences, Aug. 2003.

[14]Jorba, À., "A Methodology for the Numerical Computation of Normal Forms, Centre Manifolds and First Integrals of Hamiltonian Systems," *Experimental Mathematics*, Vol. 8, No. 2, 1999, pp. 155–195.

[15]Marsden, J., *Lectures on Mechanics*, Vol. 174, London Mathematical Society Lecture Note Series, Cambridge Univ. Press, Cambridge, England, U.K., 1992, Chap. 3.

[16]Marsden, J., and Ratiu, T., *Introduction to Mechanics and Symmetry*, Vol. 17, Texts in Applied Mathematics, 2nd ed., Springer-Verlag, New York, 1999, Chaps. 5–8.

[17]Marsden, J., Ratiu, T., and Scheurle, J., "Reduction Theory and the Lagrange-Routh Equations," *Journal of Mathematical Physics*, Vol. 41, No. 6, 2000, pp. 3379–3429.

[18]Sanyal, A. K., Shen, J., and McClamroch, N. H., "Dynamics and Control of an Elastic Dumbbell Spacecraft in a Central Gravitational Field," *Proceedings of 42nd Conference on Decision and Control*, 2003, pp. 2798–2803.

[19]Cronin, J., Richards, P., and Russell, L., "Some Periodic Solutions of a Four-Body Problem," *Icarus*, Vol. 3, No. 5–6, 1964, pp. 423–428.

[20]Gómez, G., Jorba, À., Masdemont, J., and Simó, C., *Dynamics and Mission Design near Libration Points. Vol. III*, Vol. 4, World Scientific Monograph Series in Mathematics, World Scientific, River Edge, NJ, 2001.

[21]Gómez, G., Jorba, À., Masdemont, J., and Simó, C., *Dynamics and Mission Design near Libration Points. Vol. IV*, Vol. 5, World Scientific Monograph Series in Mathematics, World Scientific, River Edge, NJ, 2001.

[22]Giorgilli, A., Delshams, A., Fontich, E., Galgani, L., and Simó, C., "Effective Stability for a Hamiltonian System near an Elliptic Equilibrium Point, with an Application to the Restricted Three Body Problem," *Journal of Differential Equations*, Vol. 77, No. 1, 1989, pp. 167–198.

[23]Simó, C., "Estabilitat de Sistemes Hamiltonians," *Memorias de la Real Academia de Ciencias y Artes de Barcelona*, Vol. 48, No. 7, 1989, pp. 303–348.

[24]Giorgilli, A., "Quantitative Methods in Classical Perturbation Theory," *From Newton to Chaos: Modern Techniques for Understanding and Coping with Chaos in N–Body Dynamical Systems*, edited by A. Roy and B. Steves, Plenum, New York, 1995, pp. 21–37.